Theoretical Study of the Ion−Molecule Reaction of the Vinyl Cation with Ethane

Pablo Campomanes, Dimas Suárez, and Tomás L. Sordo*

Departamento de Química Física y Analítica, Facultad de Química, Universidad de Oviedo, C/Julián Clavería, 8. 33006 Oviedo, Principado de Asturias, Spain

Received: February 17, 1999; In Final Form: May 21, 1999

An ab initio study was performed of the $C_2H_3^+ + C_2H_6$ ion−molecule reaction, which has received considerable experimental attention. The corresponding $C_4H_9^+$ potential energy surface (PES) was studied at the MP2/6-31G(d,p) level of theory, and single-point calculations on the MP2 geometries were carried out at the CCSD(T)/6-31G(d,p) and MP2/6-311+G(3df,2p) levels. According to our results, the initial interaction of ethane with the vinyl cation proceeds through a barrierless hydride transfer from C_2H_6 to give a $C_2H_4\cdots C_2H_5^+$ π-complex. This complex is located in a fluxional region of the PES corresponding to different π-$C_4H_9^+$ complexes around 60 kcal/mol under reactants. In consonance with previous experimental and theoretical work, it is observed that this region of the $C_4H_9^+$ PES is separated from the most stable $C_4H_9^+$ *tert*-butyl cation by an energy barrier of about 19 kcal/mol. Different product channels for the title reaction are accessible from the $C_4H_9^+$ π-complexes via H_2 or CH_4 elimination and fragmentation processes, the lowest energy profiles corresponding to the $C_2H_5^+$ and $C_3H_5^+$ exothermic channels. Gibbs energy reported in this work suggests that entropic contributions may play an important role to determine the ratio of the secondary ions corresponding to different product channels, in agreement with experimental results.

Introduction

The ion−molecule reactions of ethane have been studied for many years using different experimental techniques.[1−6] Although the general pattern of reactivity of ethane is the same in the different studies, the agreement of cross sections at different average ion energies is poor and there are some discrepancies between the different reports in the assignment of product−reactant sequences.[2−5]

The reaction between $C_2H_3^+$ and C_2H_6 has received considerable attention. Schissler and Stevenson[1] have measured the reaction cross section for the process $C_2H_3^+ + C_2H_6 \rightarrow C_3H_5^+ + CH_4$ occurring in a mass spectrometer at different ion energies. In their investigation with the technique of ion cyclotron resonance (ICR) spectroscopy, Wexler and Pobo[3] have reported three exothermic channels producing $C_2H_5^+$, $C_3H_5^+$ and $C_4H_7^+$, and two endothermic channels producing $C_3H_6^{\bullet+}$ and $C_3H_7^+$ with reaction enthalpies of 14 and 31 kcal/mol, respectively. McAllister[4] has also observed the reaction producing $C_3H_5^+$. Kim, Anicich, and Huntress[5] using both ICR and photoionization mass spectrometer methods, observed the three exothermic channels $C_2H_5^+$, $C_3H_5^+$, and $C_4H_7^+$, the first two being the major reaction channels, in agreement with the results obtained with Blair et al.[6] The ΔH values reported for these exothermic reaction channels are, respectively, −16, −51, and −46 kcal/mol.[5]

The detection and study of the *tert*-butyl and 2-butyl cations both in the gas phase and in solution have increased the understanding of chemical processes that involve the participation of carbocation intermediates in organic chemistry.[7] Auloos et al.[8] have demonstrated that the gas-phase reaction $C_2H_3^+ + C_2H_6 \rightarrow C_4H_9^+$ leads predominantly to the formation of *tert*-butyl ions in the presence of added $(CD_5)_2CDCD_3$. These authors discounted the importance of $C_2H_5^+$ ion formation in their radiolysis experiments. Tedder and co-workers[9] have also reported the formation of an initial "addition complex" $C_4H_9^+$ in the reactions of ethyl cation and ethylene, and of methyl cations and propylene. In practice the two reactions yield almost the same fragmentation ions, but the ratio of these secondary ions is different. The collision-induced decomposition (CID) spectrum of $C_4H_9^+$ ions colliding with molecular nitrogen shows two principal fragmentation routes: $C_3H_5^+$ (0.6) and $C_2H_5^+$ (0.4).

The high relative stability of the *tert*-butyl cation has been evident from the initial studies by Olah and co-workers.[10] According to NMR and photoelectron spectroscopy experiments,[11] 2-butyl cations present a rapid isomerization between a symmetrically hydride-bridged form and a second unsymmetrical structure. The 2-butyl cation can also rearrange to the most stable *tert*-butyl cation with an experimental activation energy of around 18 kcal/mol.[12] The observation of this rearrangement process in the gas phase by Shold and Ausloos[13] has clearly determined that the extent of this rearrangement depends on the fraction of the initially formed ions with sufficient internal energy to overcome the energy barrier. Previous theoretical work[14,15] on the $C_4H_9^+$ cation has provided structures and energies for the various $C_4H_9^+$ isomers and details of the mechanisms for their rearrangement, complementing thus the experimental data.[10−13]

To our knowledge, there are no previous theoretical studies on the different reaction channels and possible mechanisms for the ion−molecule reaction between the vinyl cation and ethane. Since a detailed study of the most significant stable structures and transition structures (TSs) connecting them on the $C_4H_9^+$ PES seems valuable for getting a deeper knowledge of the features determining their dynamical behavior and for understanding the experimental findings, in this work we undertook an ab initio MO investigation of the mechanism of the most

* To whom correspondence should be addressed. E-mail: tsg@dwarf1.quimica.uniovi.es.

10.1021/jp990608y CCC: $18.00
Published on Web 07/14/1999

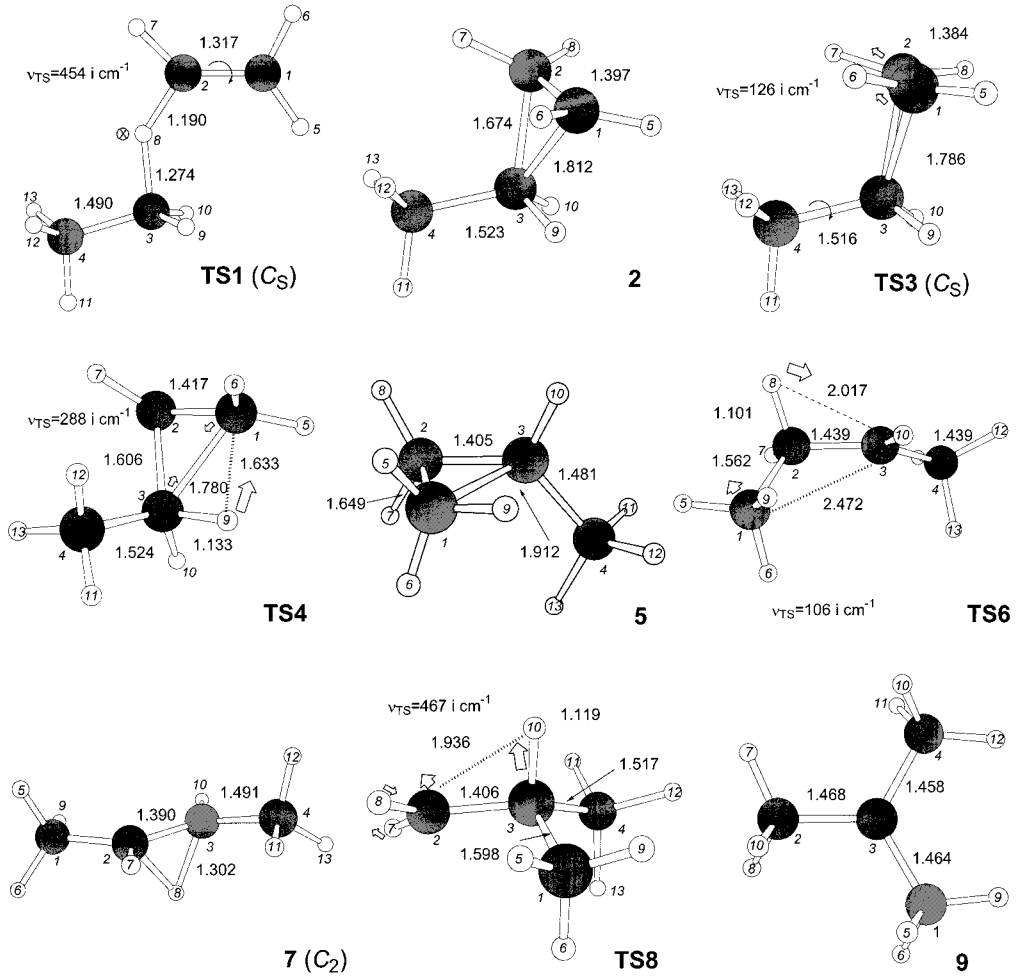

Figure 1. MP2/6-31G(d,p) optimized geometries of the TSs and intermediates located for the formation of $C_4H_9^+$ intermediates in the title reaction. Bond lengths are given in angstroms. Hollow arrows sketch the main components of the corresponding transition vectors.

important product channels for the title reaction and the related rearrangement processes on the $C_4H_9^+$ PES.

Methods of Calculation

Ab initio calculations were carried out with the Gaussian 94 series of programs.[16] Stable species were fully optimized and TSs located using Schlegel's algorithm[17] at the MP2/6-31G-(d,p) theory level.[18] All the critical points were further characterized, and the zero-point vibrational energy (ZPVE) was evaluated by analytical MP2/6-31G(d,p) computations of harmonic frequencies. In addition, CCSD(T)/6-31G(d,p) single-point calculations were carried out on the MP2/6-31G(d,p) geometries in order to estimate the effect of more elaborate *N*-electron treatments on the calculated relative energies.[19] Similarly, the influence of large basis sets on the relative energies of the MP2/6-31G(d,p) optimized structures was estimated by means of single-point MP2 calculations using the 6-311+G(3df,2p) basis set. The frozen core approximation was used in all the calculations.

Thermodynamic gas-phase data (300 and 700 K, 1 bar) were computed to obtain results more readily comparable with experimental results within the ideal gas, rigid rotor, and harmonic oscillator approximations.[20]

Reaction paths passing through the main TSs located in this work were studied by MP2/6-31G(d,p) intrinsic reaction coordinate (IRC) calculations using the Gonzalez and Schlegel method[21] implemented in Gaussian 94. Atomic charges were computed by carrying out a natural population analysis[22] (NPA) on the corresponding MP2/6-31G(d,p) density matrices.

Results and Discussion

We will investigate the most important reaction channels for the reaction of the vinyl cation with ethane. Figures 1 and 2 display the optimized geometry of the minima and TSs for the formation and interconversion of different $C_4H_9^+$ intermediate structures and of the TSs for the elimination of H_2 or CH_4 along the exothermic product channels, respectively. Table 1 presents the relative energies for the different TSs and intermediates involved in the formation and evolution of the $C_4H_9^+$ intermediate species, while Table 2 contains the corresponding reaction energies and thermodynamic data for the different product channels studied in this work. Finally, Figure 3 shows the resultant energy profile for the reaction of $C_2H_3^+$ with C_2H_6.

Unless otherwise stated, all the relative energies given in the text were computed using electronic energies approximated in an additive fashion[23] as follows:

$$E[\text{CCSD(T)/6-311+G(3df,2p)}] \approx E[\text{CCSD(T)/6-31G(d,p)}] + E[\text{MP2/6-311+G(3df,2p)}] - E[\text{MP2/6-31G(d,p)}]$$

and including the ZPVE correction from MP2/6-31G(d,p) unscaled frequencies. Thermodynamic data in Tables 1 and 2 were obtained by adding the MP2/6-31G(d,p) thermal corrections to the composite electronic energies.

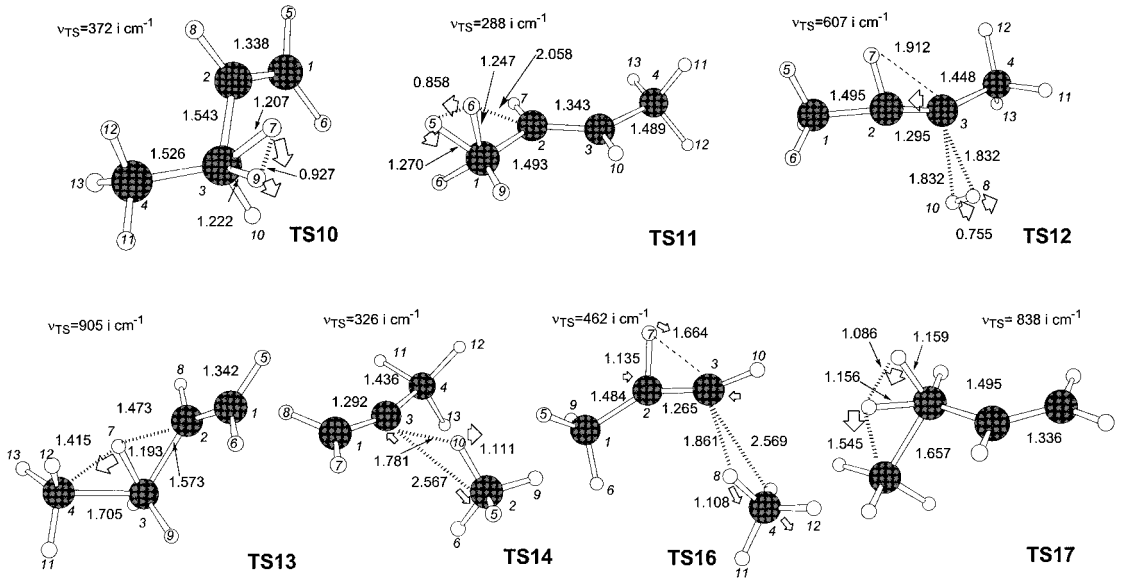

Figure 2. MP2/6-31G(d,p) optimized geometries of the TSs located in this work for CH_4 and H_2 elimination processes. Bond lengths are given in angstroms. Hollow arrows sketch the main components of the corresponding transition vectors.

TABLE 1: Relative Energies (kcal/mol) at Various Theory Levels of the Chemically Important Structures Located on the Different Reaction Channels Corresponding to the $C_2H_3^+ + C_2H_6$ Ion−Molecule Reaction in the Gas Phase[a]

structure		MP2/ 6-31G(d,p)	ZPVE[b]	CCSD(T)/ 6-31G(d,p)[c]	MP2/6-311 +G(3df,2p)[c]	ΔE[d]	ΔH[e] 300 K	ΔH[e] 700 K	ΔG[e] 300 K	ΔG[e] 700 K
$C_2H_5^+\cdots C_2H_4$, C_s	**TS1**	−23.3	2.9	−26.1	−23.1	−23.0	−24.0	−24.0	−13.1	1.6
$C_2H_5^+\cdots C_2H_4(\pi)$	**2**	−62.9	6.8	−60.8	−62.1	−53.2	−54.4	−54.5	−42.1	−25.3
$C_2H_5^+\cdots C_2H_4(\pi)$, C_s	**TS3**	−62.2	6.7	−60.3	−61.8	−53.2	−55.0	−55.8	−41.8	−23.6
TS, $C_2H_5^+\cdots C_2H_4(\pi) \rightarrow CH_3CH{=}CHCH_3\cdots H^+(\pi)$	**TS4**	−62.8	6.5	−60.5	−61.8	−53.1	−54.8	−55.8	−41.7	−23.4
$CH_3CH{=}CH_2\cdots CH_3^+(\pi)$	**TS5**	−70.1	6.7	−68.6	−69.2	−61.0	−62.4	−62.4	−50.2	−33.6
TS, $CH_3CH{=}CHCH_3\cdots H^+(\pi) \rightarrow CH_3CH{=}CH_2\cdots CH_3^+(\pi)$	**TS6**	−65.5	4.8	−66.2	−63.6	−59.5	−60.6	−61.2	−48.2	−31.1
$CH_3CH{=}CHCH_3\cdots H^+(\pi)$	**7**	−68.7	5.2	−68.1	−67.5	−61.7	−62.8	−62.9	−50.7	−34.7
TS, $CH_3CH{=}CH_2\cdots CH_3^+(\pi) \rightarrow (CH_3)_3C^+$	**TS8**	−47.7	5.2	−48.8	−45.7	−41.6	−43.1	−43.6	−30.7	−13.7
$(CH_3)_3C^+$	**9**	−79.3	4.4	−79.7	−77.4	−73.4	−75.1	−76.4	−63.7	−47.5
TS, $C_2H_5^+\cdots C_2H_4(\pi) \rightarrow CH_2CHCHCH_3^+ + H_2$	**TS10**	−23.3	3.1	−22.6	−25.3	−21.5	−22.7	−23.0	−10.5	6.3
TS, $CH_3CH{=}CH_2\cdots CH_3^+(\pi) \rightarrow CH_2CCH_2CH_3^+ + H_2$	**TS11**	−23.0	2.8	−22.6	−26.0	−22.8	−24.1	−24.3	−12.1	4.3
TS, $CH_3CH{=}CHCH_3\cdots H^+(\pi) \rightarrow CH_3CHCCH_3^+ + H_2$	**TS12**	−15.9	−0.5	−18.2	−17.7	−20.6	−21.4	−20.2	−10.4	4.0
TS, $C_2H_5^+\cdots C_2H_4(\pi) \rightarrow CH_2CHCH_2^+ + CH_4$	**TS13**	−23.6	3.5	−22.0	−24.8	−19.8	−21.0	−21.2	−9.1	7.1
TS, $CH_3CH{=}CH_2\cdots CH_3^+(\pi) \rightarrow CH_3C{=}CH_2^+\cdots CH_4$	**TS14**	−27.2	1.4	−30.1	−27.5	−29.0	−29.5	−28.8	−19.4	−6.2
$CH_3C{=}CH_2^+\cdots CH_4$	**15**	−29.2	0.4	−32.5	−29.0	−31.9	−31.2	−24.4	−29.3	−16.2
TS, $CH_3CH{=}CHCH_3\cdots H^+(\pi) \rightarrow CH_3C{=}CH_2^+ + CH_4$	**TS16**	−15.4	0.7	−17.8	−16.1	−17.7	−17.8	−16.9	−9.2	2.0
TS, $CH_2CHCHCH_3^+ + H_2 \rightarrow CH_2CHCH_2^+ + CH_4$	**TS17**	−19.7	3.2	−18.7	−22.6	−18.5	−19.6	−19.8	−7.8	8.4

[a] The values are given with respect to $C_2H_3^+(\pi) + C_2H_6$ separate fragments. [b] ZPVE correction from MP2/6-31G(d,p) frequencies. [c] Single-point calculations on the MP2/6-31G(d,p) geometries. [d] E[CCSD(T)/6-31G(d,p)] + E[MP2/6-311+G(3df,2p)] − E[MP2/6-31G(d,p)] + ZPVE[MP2/6-31G(d,p)]. [e] Thermodynamic data (1 atm) computed from MP2/6-31G(d,p) thermal corrections and the composite electronic energies.

TABLE 2: Reaction Energies (kcal/mol) of the Various Reaction Channels Considered in This Work for the $C_2H_6 + C_2H_3^+$ Ion−Molecule Reaction[a]

reaction channels	MP2/ 6-31G(d,p)	ZPVE[b]	CCSD(T)/ 6-31G(d,p)[c]	MP2/6-311 +G(3df,2p)[c]	ΔE_{rxn}[d]	ΔH_{rxn}[e] 300 K	ΔH_{rxn}[e] 700 K	ΔG_{rxn}[e] 300 K	ΔG_{rxn}[e] 700 K
$CH_3CH_2^+ + C_2H_4$	−17.3	1.6	−20.1	−17.4	−18.6	−18.8	−19.5	−18.4	−17.4
$CH_2{=}CH{-}CH{-}CH_3^+ + H_2$	−41.7	−2.3	−42.7	−39.0	−42.2	−41.4	−41.0	−38.3	−35.5
$CH_3{-}CHC{-}CH_3^+ + H_2$	−22.6	−4.6	−21.2	−23.6	−26.8	−25.6	−23.8	−23.5	−21.7
$CH_2{-}CH{-}CH_2^+ + CH_4$	−40.6	2.4	−43.0	−37.1	−37.1	−37.2	−37.4	−36.6	−35.8
$CH_2{=}C{-}CH_3^+ + CH_4$	−26.6	0.6	−30.0	−25.3	−28.1	−28.8	−28.5	−29.3	−30.1
$CH_3{-}CH{-}CH_3^+ + {}^1[{:}CH_2]$	59.0	−2.7	50.8	58.1	47.2	47.7	48.3	47.6	47.1
$CH_3^+ + CH_2{=}CH{-}CH_3$	19.1	1.0	15.9	20.2	18.0	18.4	18.2	18.6	19.0
$CH_2{=}CH{-}CH_3^{\bullet+} + CH_3^{\bullet}$	18.9	2.5	14.9	21.6	20.1	16.8	17.5	15.9	14.3

[a] The values are given with respect to the $C_2H_3^+(\pi) + C_2H_6$ separate fragments. [b] ZPVE correction from MP2/6-31G(d,p) frequencies. [c] Single-point calculations on the MP2/6-31G(d,p) geometries. [d] E[CCSD(T)/6-31G(d,p)] + E[MP2/6-311+G(3df,2p)] − E[MP2/6-31G(d,p)] + ZPVE[MP2/6-31G(d,p)]. [e] Thermodynamic data (1 atm) computed from the MP2/6-31G(d,p) thermal corrections and the composite electronic energies.

Isomers of the Vinyl Cation $C_2H_3^+$. To calibrate the methodology to be used in the determination of the energetics as well as the mechanism of the title reaction, the electronic energy differences between the different isomers of $C_2H_3^+$ were also calculated in this work at the CCSD(T)/6-311+G(3df,2p) level using the corresponding MP2/6-311+G(3df,2p) geom-

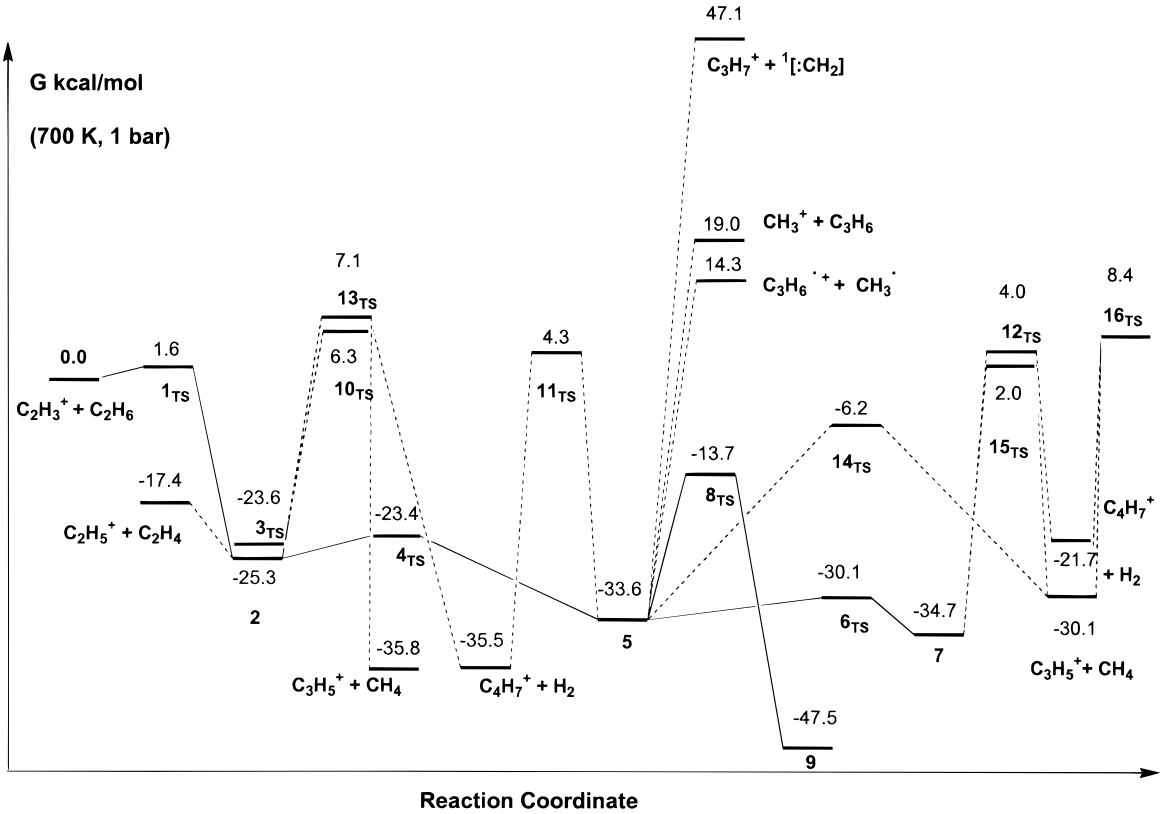

Figure 3. Energy profiles for the possible reaction channels corresponding to the reaction of the $C_2H_3^+$ cation and ethane. ZPVE corrections were computed using the MP2/6-31G(d,p) analytical frequencies, while electronic energies were calculated in an additive manner (see text for the details).

etries. At this level of theory, the nonclassical structure (π-complex) is the most stable $C_2H_3^+$ isomer, 3.8 and 49.3 kcal/mol under the other two isomeric structures, the σ-cation CH_2-CH^+ and the methylcarbine cation CH_3C^+, respectively (MP2/6-311+G(3df,2p) frequencies characterize the CH_2CH^+ structure as a first-order saddle point).[24] Our theoretical calculations using the additive scheme shown above give for these electronic energy gaps 3.7 and 49.4 kcal/mol, respectively, differing in only 0.1 kcal/mol from the CCSD(T) ones. All the relative energies in this work are given with respect to the most stable π-cation isomer of $C_2H_3^+$.

Formation of the Initial Addition Complex $C_4H_9^+$. According to reaction coordinate calculations along a C_s least-motion approach, the initial interaction between the $C_2H_3^+$ cation and C_2H_6 proceeds through a barrierless hydride shift from C_2H_6 to give a bridged $C_4H_9^+$ complex (**TS1** in Figure 1), which can be considered as the minimum energy point along the reaction trajectory for the indicated H-shift.[25] This complex of C_s symmetry presents a H atom of the C_2H_4 moiety situated in a bridged position interacting with a C atom of the $C_2H_5^+$ moiety and is 23.0 kcal/mol more stable than separate reactants. According to NPA charges, a notable charge transfer (0.52 e) from the ethylene moiety to the ethyl cation stabilizes this complex. Nevertheless, analytical frequencies and IRC calculations confirm that **TS1** is not a stable structure on the MP2/6-31G(d,p) PES (see Figure 3) but is a first-order saddle point possessing an imaginary frequency (454i cm^{-1}) that corresponds to an internal torsional motion to give a π-complex between C_2H_4 and $C_2H_5^+$ (**2** in Figure 1), which is 53.2 kcal/mol more stable than separate reactants. Therefore, the existence of the bridged $C_4H_9^+$ complex **TS1** can only be transient.[25]

The π-complex $C_4H_9^+$, **2**, which can be also seen as a corner-protonated methylcyclopropene, has C_1 symmetry and presents two different C−C bonds with bond lengths of 1.674 and 1.812 Å, while the NPA charge transfer from ethylene to the ethyl cation increases 0.10 e with respect to the TS structure **TS1**. A C_s π-complex between C_2H_4 and $C_2H_5^+$ (**TS3** in Figure 1) was also located on the PES, presenting a C−C bond length and a charge transfer of 1.786 Å and 0.53 e, respectively. The symmetrical structure **TS3** results in a TS on the MP2/6-31G-(d,p) PES for the isomerization of **2** to its mirror image (see Figure 3). This isomerization of the π-complex **2** passing through a symmetrical π-complex has a very low energy barrier of 0.7 kcal/mol at the MP2/6-31G(d,p) level, but the best theory level using the above-mentioned additive scheme renders it as a fluxional motion without any energy barrier (see Table 1).

The initial intermediate $C_4H_9^+$, **2**, can evolve easily through a TS (**TS4** in Figure 1) for a 1,3-H shift from the ethyl cation moiety to the ethylene fragment to give another $C_4H_9^+$ minimum on the PES resembling a corner-protonated methylcyclopropane (**5** in Figure 1), which is 7.8 kcal/mol more stable than intermediate **2**. The energy barrier for this proton-scrambling process is only 0.1 kcal/mol with respect to **2**. According to its structure, **5** is best described as a π-complex between a CH_3^+ moiety and propylene with two asymmetrical C−C bonds with bond lengths of 1.649 and 1.912 Å and an NPA charge transfer from propylene to the methyl cation of 0.70 e.

The π-complex **5** can readily evolve to another $C_4H_9^+$ intermediate (**7** in Figure 1), 0.7 kcal/mol more stable than **5,** through a TS with an energy barrier of only 1.5 kcal/mol (**TS6** in Figure 1). The nature of this TS was further confirmed using IRC reaction coordinate calculations. The structure **7** corresponds to the H-bridged 2-butyl cation of C_2 symmetry in which the proton is symmetrically attached to the double bond through a C−H bond length of 1.302 Å and accommodates an NPA population of 0.59 e. The calculated energy profile in Figure 3 manifests a satisfactory agreement with the most recent experimental data indicating that the symmetrical 2-butyl cation **7** is

in fast equilibrium at low temperatures with a second unsymmetrical structure, the H-bridged form being more stable by 0.4 kcal/mol.[11a,14]

When the CH_3^+ fragment in complex **5** becomes attached to the central C atom of the propylene moiety with simultaneous 1,2-migration of a H atom through the TS structure **TS8**, structure **5** evolves to give the most stable $C_4H_9^+$ intermediate **9**, the $(CH_3)_3C^+$ *tert*-butyl cation of C_1 symmetry,[14] which is 73.4 kcal/mol more stable than separate reactants (see Figure 3). Figure 1 shows that **TS8** resembles a primary isobutyl carbocation, which is not a stable minimum on the PES.[15] The energy barrier associated with the formation of the $(CH_3)_3C^+$ cation from its immediate $C_4H_9^+$ precursor **5** is 19.4 kcal/mol, the $(CH_3)_3C^+$ cation being around 12 kcal/mol more stable than intermediates **5** and **7**. These energy values are very close to those reported in earlier theoretical work.[14,15] The experimental values are 18.0 and 14−16 kcal/mol for the activation and reaction energies, respectively.[12,26]

Therefore, the relatively complex $C_4H_9^+$ energy profile obtained with our calculations shows two clearly distinct zones (see Figure 3). The first one is a fluxional region of the PES corresponding to different π-$C_4H_9^+$ complexes, around 60 kcal/mol under reactants, which are very easily interconnected through very low energy barriers that facilitate a full proton scrambling between the initial reactants. This minimum energy area would correspond to the initial addition complex reported by experimentalists[9] and is clearly separated through a notable energy barrier of around 19 kcal/mol from the most stable $C_4H_9^+$ *tert*-butyl cation constituted by a unique σ bond C−C skeleton.

Exothermic Channels $C_2H_5^+$, $C_4H_7^+$, and $C_3H_5^+$. According to reaction coordinate calculations on the MP2/6-31G(d,p) PES by varying the appropriate C−C distances, the formation of the ethyl cation in the $C_2H_3^+ + C_2H_6$ ion−molecule process may easily proceed through a barrierless rupture of the $C_4H_9^+$ intermediate **2** into the $C_2H_5^+$ and C_2H_4 products. As previously mentioned, **2** can be best considered as a π-complex between ethylene and the ethyl cation, the binding energy of this complex being 34.6 kcal/mol while the $C_2H_5^+$ and C_2H_4 separate products are 18.6 kcal/mol more stable than the initial reactants (see Table 2). This calculated exoergicity presents a satisfactory agreement with the reported experimental ΔH value for the $C_2H_3^+ + C_2H_6 \rightarrow C_2H_5^+ + C_2H_4$ process (−16 kcal/mol).[5]

Concerning the formation of the $C_4H_7^+$ cation, we found three different TSs for H_2 elimination from the $C_4H_9^+$ intermediate structures **2**, **5**, and **7**. From **2** a H_2 elimination occurs through a TS structure (**TS10** in Figure 2) in which the atoms of the emerging H_2 molecule present a three-center interaction[27] with a carbon atom with two C−H distances of 1.207 and 1.222 Å and a H−H distance of 0.927 Å. IRC calculations confirm that **TS10** corresponds to a 1,2-H_2 elimination process to give a methylallyl cation. The calculated energy barrier for **TS10** with respect to the previous complex **2** presents a value of 31.7 kcal/mol, while the $CH_3-CH-CH-CH_2^+ + H_2$ separate products are 42.2 kcal/mol more stable than the initial reactants (11.0 kcal/mol less stable than **2**; see Tables 1 and 2).

TS11 in Figure 2 is the TS for the 1,2-H_2 elimination process from **5**. In **TS11**, the three-membered ring in **5** is opened and a methylene H atom in the propylene moiety forms a three-center interaction with another H atom from the terminal methyl group (see Figure 2). Our calculations render a comparable energy and structure for both **TS10** and **TS11**, the later one being only 1.3 kcal/mol more stable and presenting an energy barrier with respect to its $C_4H_9^+$ precursor of 38.2 kcal/mol.

$C_4H_7^+$ can also be formed from **7** through a 1,1-H_2 elimination TS, **TS12**, which is also shown in Figure 2. IRC calculations reveal that the leaving H_2 molecule comes from the bridged H in **7** and one of the H atoms bonded to the C3 atom. **TS12** shows a symmetrical departure (C−H bond lengths = 1.832 Å) of a practically formed H_2 molecule (H−H bond length = 0.755 Å), while the hydrogen atom attached to C2 shows an initial π bond with the two central C atoms (see Figure 2). According to our calculations, 41.1 kcal/mol are required to eliminate the H_2 molecule from **7** via the *product-like* **TS12**, rendering a π-protonated 2-butine cation that is 15.4 kcal/mol less stable than the methylallyl cation. Nevertheless, this product channel is also exoergic with respect to the initial reactants given that the π-protonated butine + H_2 separate products are 26.8 kcal/mol more stable than $C_2H_3^+ + C_2H_6$.

From the above results it is clear that these energy profiles for the $C_2H_3^+ + C_2H_6 \rightarrow C_4H_7^+ + H_2$ exothermic process are below the initial reactants, the three TSs for the H_2 elimination pathways being about 20 kcal/mol more stable than reactants (see Figure 3). We also note that the calculated exoergicity of this process to give the most stable $C_4H_7^+$ cation (−42.2 kcal/mol) compares well with the reported experimental ΔH value of −46 kcal/mol. However, a prediction of the most favored mechanistic route for the $C_4H_7^+$ channel may require a study of the detailed dynamics of the processes.

The $C_4H_9^+$ intermediates **2**, **5**, and **7** can also evolve along CH_4 elimination processes leading to the formation of different $C_3H_5^+$ isomers. A methyl group and a H atom from the ethyl cation and ethylene moieties in structure **2**, respectively, can be eliminated to form a CH_4 molecule through the TS structure **TS13** (see Figure 2). The geometrical structure and the IRC reaction path for this TS are analogous to those for the 1,2-H_2 elimination **TS10**, **TS13** manifesting also a three-center interaction of the departing CH_3 group (C−C bond length of 1.705 Å) and H atom (C−H bond length of 1.193 Å) with the terminus C atom in the forming allyl cation $C_3H_5^+$ (see Figure 2). The energy barrier for the direct fragmentation of **2** into methane and the allyl cation $C_3H_5^+$ is 33.4 kcal/mol, only 1.7 kcal/mol greater than that for the 1,2-H_2 elimination. Our calculations also predict that both **TS13** and separate products ($CH_4 + C_3H_5^+$) are clearly more stable than the initial reactants ($C_2H_3^+ + C_2H_6$) by 19.8 and 37.1 kcal/mol, respectively.

As expected from the structure of **5** resembling a methyl cation forming a π-complex with the propylene moiety, this intermediate can lose a methane molecule by means of a 1,2-H migration with simultaneous rupture of two weak C−C bonds through the TS structure **TS14** in Figure 2. In **TS14**, the proton is almost transferred to the leaving CH_4 molecule, which presents a weak interaction with the central carbon atom of a quasi-formed 2-methylvinyl cation (the bond lengths of the C−H and C−C breaking bonds are 1.781 and 2.567 Å, respectively; see Figure 2). **TS14** is 9.2 kcal/mol more stable than **TS13** and has an energy barrier with respect to **5** of 32.0 kcal/mol, while the resulting 2-methylvinyl $C_3H_5^+$ cation is 9.0 kcal/mol less stable than the allyl cation. According to IRC calculations as well as MP2/6-31G(d,p) geometry optimizations, **TS14** is connected with a weak ion−molecule complex, **15** in Table 1, between methane and the 2-methylvinyl cation. This complex (not shown in Figure 2 for brevity) has C_s symmetry, an equilibrium $C(CH_4)-C_3(C_3H_5^+)$ distance of 3.187 Å and is 2.9 and 3.8 kcal/mol under **TS14** and the corresponding $CH_4 + C_3H_5^+$ products, respectively (see Figure 3). The complex **15** dissociates into the $CH_4 + C_3H_5^+$ products, 28.1 kcal/mol below the initial reactants. In a previous theoretical work,[28] a low

energy profile for the isomerization mechanism between the 2-methylvinyl cation and the allyl cation passing through a corner-protonated cyclopropene has been determined.

The π-protonated 2-butene **7** can also dissociate into a CH_4 molecule and a 2-methylvinyl $C_3H_5^+$ cation by means of a 1,1-elimination mechanism through **TS16** in Figure 2. This is a quite advanced TS in which a methane molecule is practically formed with the breaking C−H and C−C bonds presenting bond lengths of 1.861 and 2.569 Å, respectively (see Figure 2). An IRC calculation starting at **TS16** shows that this TS is connected with the $C_4H_9^+$ intermediate **7**, the transition vector for the CH_4 elimination maintaining an approximate C_s symmetry along the reaction path. The computed energy barrier and reaction energy for this 1,1-CH_4 elimination with respect to structure **7** are, respectively, 44.0 and 33.6 kcal/mol. Thus, we see in Figure 3 that all the energy profiles leading to $C_3H_5^+$ cations proceed below separate reactants, the TSs **TS13, TS14,** and **TS16** being, respectively, 19.8, 29.0, and 17.7 kcal/mol more stable than reactants. **TS16** is the least stable TS on the PES for H_2 and CH_4 elimination processes, while **TS14** is the most stable one. The computed reaction energy for the formation of the allyl cation $C_3H_5^+$ (−37.1 kcal/mol) is 14 kcal/mol lower in absolute value than the reported experimental estimation.[5] This discrepancy between the theoretical and experimental values is difficult to rationalize given that the allyl cation is the most stable $C_3H_5^+$ isomer.[28]

The $C_4H_7^+ + H_2 \rightarrow C_3H_5^+ + CH_4$ reaction can proceed through the TS structure **TS17** (see Figures 2 and 3). This saddle point, which presents a tight structure showing a three-center interaction between a H_2 moiety and a nearly tetrahedral carbon atom, can be described as a TS for the insertion of H_2 into the H_3C-C bond in the methylallyl cation $C_4H_7^+$, involving the simultaneous elimination of a CH_4 molecule to give an allyl cation $C_3H_5^+$. This is confirmed by inspection of the transition vector as well as the calculation of the IRC reaction path. **TS17** is 18.5 kcal/mol more stable than separate ethane and the $C_2H_3^+$ cation and is very close in energy to the rest of TSs in Figure 2 (see Table 2). The corresponding energy barrier with respect to separate H_2 and the methylallyl cation is 23.7 kcal/mol.

Endothermic Channels CH_3^+, $C_3H_6^{\bullet+}$, and $C_3H_7^+$. As mentioned in the Introduction, ICR experiments[2] rendered two endothermic channels producing the radical cation $C_3H_6^{\bullet+}$ and the $C_3H_7^+$ cation for the ion−molecule reaction between the vinyl cation and ethane. According to our calculations, these endothermic channels stem from structure **5**, which resembles a π-complex between CH_3^+ and propylene and therefore plays an essential role in the mechanism of the title reaction.

According to reaction coordinate calculations, the formation of the $C_3H_7^+$ cation can occur through a barrierless fragmentation[29] of the three-membered ring in **5** to give a neutral singlet carbene $^1[:CH_2]$ and a propyl cation $C_3H_7^+$, which are 47.2 kcal/mol less stable than separate reactants (see Table 2). The reaction enthalpy reported by experimentalists for this process is 31 kcal/mol.[3]

Concerning the $C_3H_6^{\bullet+} + CH_3^{\bullet}$ endothermic channel, the calculated reaction energy with respect to reactants amounts to 20.1 kcal/mol compared with the experimental ΔH reported of 14 kcal/mol. It is reasonable to expect that this product channel may be accessible from **5** by means of a homolytic rupture of its three-membered ring, forming thus a methyl radical and a propylene radical. Similarly, the heterolytic disassociation of **5** into propylene and the methyl cation is also to be expected. In this case, our reaction coordinate calculations indicate that this process may occur in a barrierless manner to yield $C_3H_6 + CH_3^+$ products, which are 18.0 kcal/mol less stable than $C_2H_3^+ + C_2H_6$.

Thermodynamic Analysis. Ion−molecule reactions are best described by performing dynamics calculations or in the realm of the variational transition-state theory.[30] To obtain an indication of the effect of temperature and entropy on the processes presented above, we calculated the enthalpies and Gibbs energies for all the structures implied at two temperatures: 300 and 700 K.

From Table 1 we see that, at 300 K, entropy destabilizes all the TSs and intermediates by about 10−11 kcal/mol except for **TS14** and, particularly, **TS16** owing to the their quite advanced structure. At 300−700 K, this destabilization is around 15−18.5 kcal/mol except for those TSs presenting the most *productlike* character: **TS12**, **TS14**, and **TS16**. As a consequence, at 700 K, all the TS structures except **TS14** are less stable than separate reactants in terms of Gibbs energy while all the $C_4H_9^+$ intermediates remain more stable than separate reactants (see Table 1).

Our ΔG values clearly yield the *tert*-butyl cation **9** as the most stable form of the $C_4H_9^+$ species, in agreement with experimental evidence.[4] Figures in Table 1 also reflect the observed preference for two exothermic fragmentation routes of the title reaction, i.e., the $C_3H_5^+$ and $C_2H_5^+$ channels. In effect, as previously discussed, the reactive complex **2**, formed through a hydrogen transfer from ethane to $C_2H_3^+$, can easily dissociate into ethylene and the $C_2H_5^+$ cation, presenting a Gibbs reaction energy of −17.4 kcal/mol at 700 K. Alternatively, **TS4** with a Gibbs activation energy at 700 K of 1.9 kcal/mol connects the intermediate **2** with the CH_3^+−propylene π-complex **5**. This π-complex can evolve through the most stable **TS14** for CH_4 elimination (ΔG(**5**→**TS14**) = 27.4 kcal/mol at 700 K). Table 1 shows an important difference in Gibbs energy, ranging from 8 to 14 kcal/mol, between **TS14** and the rest of TSs for H_2 or CH_4 elimination, **TS14** remaining more stable than separate reactants by 6.2 kcal/mol.

As expected, the influence of entropy and temperature on ΔG_{rxn} is remarkably lower (see Table 2). At 300 K all the products are destabilized by entropy except for the exothermic channel $CH_2{=}C{-}CH_3^+ + CH_4$ and for the endothermic channel $CH_2{=}CH{-}CH_3^{\bullet+} + CH_3^{\bullet}$. At 700 K the only stabilized reaction channels are $CH_3{-}CH{-}CH_3^+ + {}^1[:CH_2]$ and especially $CH_2{=}CH{-}CH_3^{\bullet+} + CH_3^{\bullet}$.

Conclusions

The energy profile displayed in Figure 3 describes various possible mechanisms for the most important reaction channels corresponding to the $C_2H_3^+ + C_2H_6$ ion−molecule reaction. The initial H-shift from C_2H_6 gives a bridged $C_4H_9^+$ complex **1**, which is a saddle point on the PES connected with π-complex **2** between C_2H_4 and $C_2H_5^+$. The barrierless dissociation of **2** into its component fragments leads to the $C_2H_5^+$ exothermic channel ($\Delta E_{rxn} = -18.6$ kcal/mol). Structures **2**−**7** characterize a fluxional region of different π-$C_4H_9^+$ complexes, which are around 60 kcal/mol under reactants, corresponding to the initial addition $C_4H_9^+$ complexes reported by experimentalists.[6] In agreement with previous theoretical and experimental work, our calculations predict that the propylene−CH_3^+ π-complex **5** is also connected with the most stable $C_4H_9^+$ *tert*-butyl cation **9** through a notable energy barrier of 19.4 kcal/mol. TSs in Figure 2 for H_2 or CH_4 elimination processes from different π-complexes are energetically more stable than reactants, although **TS14**, which describes the 1,1-CH_4 elimination from **5**, is 10

kcal/mol more stable than the rest of TSs. The inclusion of thermal corrections at 700 K renders **TS14** under reactants, whereas the remaining TSs for H_2 or CH_4 elimination processes become less stable than separate reactants in Gibbs energy in agreement with the preference for CH_4 elimination detected experimentally.[5,6] The calculated reaction energies for the exothermic reaction channels $C_2H_5^+$, $C_3H_5^+$, and $C_4H_7^+$ are −18.6, −37.1, and −42.2 kcal/mol, respectively, whereas those for the $C_3H_7^+$ and $C_3H_6^{\bullet+}$ endothermic channels are 47.2 and 18.0 kcal/mol, respectively.

Acknowledgment. The authors are grateful to the FICYT (Spain) for financial support (PBAMB9805C1). We also thank CIEMAT (Ministerio de Industria y Energia) for computer time.

References and Notes

(1) Schissler, D. O.; Stevenson, D. P. *J. Chem. Phys.* **1956**, *24*, 926.
(2) Munson, M. S. B.; Franklin, J. L.; Field, F. H. *J. Phys. Chem.* **1964**, *68*, 3098.
(3) Wexler, S.; Pobo, L. G. *J. Am. Chem. Soc.* **1971**, *93*, 1327.
(4) McAllister, T. *J. Chem. Phys.* **1972**, *56*, 5192.
(5) Kim, J. K.; Anicich, V. G.; Huntress, W. T., Jr. *J. Phys. Chem.* **1977**, *81*, 1798.
(6) Blair, A. S.; Heslin, E. J.; Harrison, A. G. *J. Am. Chem. Soc.* **1972**, *94*, 2935.
(7) Vogel, P. *Carbocation Chemistry*; Elsevier: Amsterdam, 1985.
(8) Ausloos, P.; Rebbert, R. E.; Sieck, L. W. *J. Chem. Phys*. **1971**, *54*, 2612.
(9) Batey, J. H.; Tedder, J. M. *J. Chem. Soc., Perkin Trans. 2* **1983**, 1263.
(10) Olah, G. A.; Baker, E. B.; Evans, J. C.; Tolgyosi, W. S.; McIntyre, J. S.; Bastian, I. J. *J. Am. Chem. Soc*. **1964**, *86*, 1360.
(11) (a) Johnson, S. A.; Clark, D. T. *J. Am. Chem. Soc.* **1988**, *110*, 4112. (b) Saunders, M.; Hagen, E. L.; Rosenfeld, J. *J. Am. Chem. Soc*. **1968**, *90*, 6882.
(12) Prakash, G. K. S.; Husain, A.; Olah, G. A. *Angew. Chem.* **1983**, *95*, 51.
(13) (a) Shold, D. M.; Ausloos, P. *J. Am. Chem. Soc.* **1978**, *100*, 7915. (b) Lias, S. G.; Rebbert, R. E.; Ausloos, P. *J. Am. Chem. Soc*. **1970**, *92*, 6430.
(14) Sieber, S.; Buzek, P.; Schleyer, P. v. R.; Koch, W.; Carneiro, J. W. M. *J. Am. Chem. Soc*. **1993**, *115*, 259 and references therein.
(15) Boronat, M.; Viruela, P.; Corma, A. *J. Phys. Chem.* **1996**, *100*, 633.
(16) Frisch, M. J.; Trucks, G. W.; Schlegel, H. B.; Gill, P. M. W.; Johnson, B. G.; Robb, M. A.; Cheesman, J. R.; Keith, T. A.; Petersson, G. A.; Montgomery, J. A.; Raghavachari, K.; Al-Lahan, M. A.; Zakrzewski, V. G.; Ortiz, J. V.; Foresman, J. B.; Cioslowski, J.; Stefanov, B. B.; Nanayakkara, A.; Challacombe, M.; Peng, C. Y.; Ayala, P. Y.; Chen, W.; Wong, M. W.; Andres, J. L.; Replogle, E. S.; Gomperts, R.; Martin, R. L.; Fox, D. J.; Binkley, J. S.; Defrees, D. J.; Baker, J.; Stewart, J. P.; Head-Gordon, M.; Gonzalez, C.; Pople, J. A. *Gaussian 94*; Gaussian, Inc.: Pittsburgh, PA, 1995.
(17) Schlegel, H. B. *J. Comput. Chem.* **1982**, *3*, 211
(18) Hehre, W. J.; Radom, L.; Pople, J. A.; Schleyer, P. v. R. *Ab Initio Molecular Orbital Theory*; John Wiley & Sons Inc.: New York, 1986.
(19) Bartlett, R. J. *J. Phys. Chem.* **1989**, *93*, 1697.
(20) McQuarrie, D. A. *Statistical Mechanics*; Harper & Row: New York, 1976.
(21) (a) Fukui, K. *Acc. Chem. Res.* **1981**, *14*, 363. (b) Gonzalez, C.; Schlegel, H. B. *J. Phys. Chem*. **1989**, *90*, 2154. (c) Gonzalez, C.; Schlegel, H. B. *J. Phys. Chem.* **1990**, *94*, 5523.
(22) Reed, A. E.; Weinstock, R. B.; Weinhold, F. *J Chem. Phys.* **1985**, *83*, 735.
(23) Curtiss, L. A.; Redfem, P. C.; Smith, B. J.; Radom, L. *J. Chem. Phys*. **1996**, *104*, 5148.
(24) (a) del-Río, E.; López, R.; Sordo, T. L. *J. Phys. Chem. A* **1998**, *102*, 6831. (b) Maluendes, S. A.; McLean, A. D.; Herbst, E. *Chem. Phys. Lett.* **1994**, *217*, 571. (c) Lee, T. J.; Schaefer, H. F. *J. Chem. Phys.* **1986**, *86*, 3437.
(25) Uggerud, E. *J. Am. Chem. Soc*. **1994**, *116*, 6873.
(26) (a) Schultz, J. C.; Houle, F. A. *J. Am. Chem. Soc*. **1984**, *106*, 3917. (b) Lias, S. G.; Shold, D. M.; Ausloos, P. *J. Am. Chem. Soc*. **1980**, *102*, 2540.
(27) Suárez, D.; Sordo, T. L. *J. Phys. Chem. A* **1997**, *101*, 1561.
(28) López, R.; Sordo, J. A.; Sordo, T. L.; Schleyer, P. v. R. *J. Comput. Chem.* **1996**, *17*, 905.
(29) Díaz, N.; Suárez, D.; Sordo, T. L. *J. Phys. Chem. A* **1998**, *102*, 9918.
(30) Truhlar, D. G.; Garret, B. E.; Kilppenstein, S. J. *J. Phys. Chem.* **1996**, *100*, 12771.